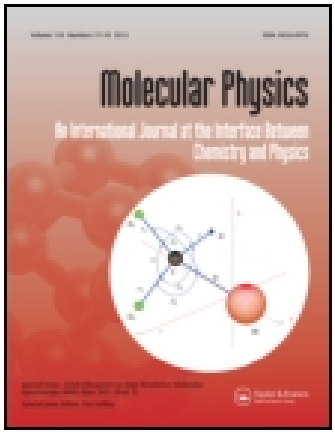

Molecular Physics: An International Journal at the Interface Between Chemistry and Physics
Publication details, including instructions for authors and subscription information:
http://www.tandfonline.com/loi/tmph20

Low-pressure line shape study of acetylene transitions in the $\nu_1+\nu_2+\nu_4+\nu_5$ band over a range of temperatures

Chad Povey [a], Adriana Predoi-Cross [a] & Daniel R. Hurtmans [b]

[a] Alberta Terrestrial Imaging Centre, Department of Physics and Astronomy, University of Lethbridge, 4401 University Drive, Lethbridge, AB, T1K 3M4 Canada

[b] Service de Chimie Quantique et Photophysique CP 160/09, Université Libre de Bruxelles, 50, Av. Roosevelt, B-1050 Bruxelles, Belgium

Accepted author version posted online: 09 Jul 2012.Published online: 10 Aug 2012.

To cite this article: Chad Povey, Adriana Predoi-Cross & Daniel R. Hurtmans (2012) Low-pressure line shape study of acetylene transitions in the $\nu_1+\nu_2+\nu_4+\nu_5$ band over a range of temperatures, Molecular Physics: An International Journal at the Interface Between Chemistry and Physics, 110:21-22, 2633-2644, DOI: 10.1080/00268976.2012.705908

To link to this article: http://dx.doi.org/10.1080/00268976.2012.705908

Molecular Physics
Vol. 110, Nos. 21–22, November 2012, 2633–2644

Taylor & Francis
Taylor & Francis Group

SPECIAL ISSUE: FASE (FEMTO-, ASTRO-, SPECTRO-ETHYNE)

Low-pressure line shape study of acetylene transitions in the $\nu_1 + \nu_2 + \nu_4 + \nu_5$ band over a range of temperatures

Chad Povey[a], Adriana Predoi-Cross[a]* and Daniel R. Hurtmans[b]

[a]*Alberta Terrestrial Imaging Centre, Department of Physics and Astronomy, University of Lethbridge, 4401 University Drive, Lethbridge, AB, T1K 3M4 Canada;* [b]*Service de Chimie Quantique et Photophysique CP 160/09, Université Libre de Bruxelles, 50, Av. Roosevelt, B-1050 Bruxelles, Belgium*

(*Received 19 May 2012; final version received 19 June 2012*)

In this study we have retrieved the self-broadened widths, self-pressure-induced shifts, and Dicke narrowing coefficients for 20 R-branch transitions in the $\nu_1 + \nu_2 + \nu_4 + \nu_5$ band of acetylene. The spectra were recorded using a three-channel diode laser spectrometer, a temperature-controlled cell of fixed length and a second, room temperature cell. The soft collision (Galatry) and hard collision (Rautian) profiles with inclusion of line mixing effects were used to retrieve the line parameters. We determined the temperature dependencies for line broadening, shift, and Dicke narrowing coefficients. We performed comparisons between our retrieved line parameters and published line parameters for acetylene transitions.

Keywords: temperature variable cell; absorption; control software; laser spectroscopy; acetylene; spectral line shapes; intensities; pressure broadening; pressure-induced shifts; infrared spectroscopy; remote sensing; spectral line parameters

1. Introduction

The acetylene molecule can be found as a trace constituent in many atmospheres containing hydrocarbons. In particular, acetylene has been found in the atmospheres of Titan, Saturn and Jupiter [1–5]. It has also been found to be an important contributor to Earth's atmospheric chemistry as a result of anthropogenic influences [6–9]. An improved understanding of the spectral line parameters for acetylene is needed to improve the atmospheric models used to describe the above atmospheric systems. In particular, a more complete understanding of how acetylene spectral line parameters vary with temperature and pressure is required.

To date, an extensive set of measurements for spectral line parameters have been made over several vibrational bands. One of the early studies was completed by Varanasi and Bangaru [10]. The authors examined both self- and H_2-broadening in the $\nu_1 + \nu_3$ band. This band was also studied by Minutolo *et al*. [11] and Li *et al*. [12]. The study of Minutolo *et al*. [11] also covered measurements of the $\nu_1 + \nu_3 + \nu_4 - \nu_4$ and $\nu_1 + \nu_3 + \nu_5 - \nu_5$ bands. For the $\nu_4 + \nu_5$ band, two studies were completed by Lepère *et al*. [13] and Dhyne *et al*. [14]. There have been a total of five studies that examined line parameters in the $\nu_1 + 3\nu_3$ band [15–19]. A set of seven bands, which include the $3\nu_5$, $(2\nu_4 + \nu_5)$I, $(2\nu_4 + \nu_5)$II, $\nu_2 + \nu_3$, $\nu_1 + (2\nu_4 + \nu_5)$I, $\nu_2 + \nu_3 + \nu_4$ and $\nu_1 + \nu_3 - \nu_4$, were examined in two published studies by Jacquemart *et al*. [20,21]. The $5\nu_3$ band has been examined by both Wong [22] and Georges *et al*. [23]. Spectral line parameters of the $\nu_1 + \nu_5$, ν_5 and $\nu_1 + \nu_2 + \nu_4 + \nu_5$ band have been studied by Pine [24], Lambot *et al*. [25] and Povey *et al*. [26], respectively.

The motivation for the work presented here stems from the lack of temperature-dependent studies that have been completed for the acetylene molecule. One of the first studies to examine low-temperature broadening was the work completed by Lambot *et al*. [25]. Later work completed by both Dhyne *et al*. [14] and Povey *et al*. [26] examined the temperature dependencies of both self-broadening and self-shift. Of the works mentioned above, several suggest the need for a diffusion line shape model when examining spectra at pressures below 100 Torr [12,14,16,19,27]. The studies completed by both Herregodts *et al*. [16] and Valipour *et al*. [19] examined the narrowing coefficients for both hard and soft collision line shape models at room temperature. However, to date there has been no complete study of the narrowing coefficient and its temperature dependence.

*Corresponding author. Email: adriana.predoicross@uleth.ca

ISSN 0026–8976 print/ISSN 1362–3028 online

http://dx.doi.org/10.1080/00268976.2012.705908
http://www.tandfonline.com

2. Experimental details

Spectra of C_2H_2 were recorded using the three-channel tunable diode laser system developed at the University of Lethbridge [26]. The system uses a New Focus Velocity laser system tunable between 1500 and 1570 nm and operates with a $S/N > 1000$. Two sample chambers are used for this system: the first is a variable temperature controlled cell of 1.54 m length and the second a room temperature cell of similar length. Further details of the experimental setup can be found in Ref. [26].

To complete a careful examination of the temperature dependence for self-shift, self-broadening and narrowing coefficients, we recorded spectra for the R(0) to R(19) transitions of the $\nu_1 + \nu_2 + \nu_4 + \nu_5$ band using C_2H_2 provided by Praxair with a quoted purity of 99.6%. For each line we recorded spectra at six separate pressures: 10, 25, 40, 65, 90, and 115 Torr and at seven different temperatures: 213, 233, 253, 273, 293, 313, and 333 K. Table 1 shows the experimental conditions for each scan completed. The pressures were recorded using an MKS capacitance monometer with a full range of 100 (±0.1%) Torr and monitored by a signal conditioner model 670. The low gas pressures from the second channel of the spectrometer were recorded using a MKS capacitance manometer with a full range of 10 Torr. The temperatures were recorded using five platinum thermal resistors mounted on rods of different length and monitored by an eight-channel Lakeshore (model 218) temperature monitor. The errors and temperature stability associated with our temperature measurements were discussed in our previous publication [26].

For each of the measured transitions we recorded three spectra. The first spectrum was the absorption of the radiation along the temperature-controlled path. The second was a low-pressure room temperature measurement of the same transition used to determine accurately the pressure-induced shift. The third spectrum was the base background used to create the transmission profile. A fourth simultaneous measurement was also made using a Fabry Perot cavity with a free spectral range of $0.05\,cm^{-1}$. The fourth measurement is necessary to correct for the nonlinear nature of the piezoelectric device inside the laser system, and to provide accurate wavelength readings.

We examined the instrumental line shape (ILS) for our diode laser spectrometer. Prior to the analysis of our data we recorded five room temperature spectra of the R(19), R(18), P(21), P(20), and P(11) transitions in the $\nu_1 + \nu_3$ band of acetylene. The spectra were recorded in the Doppler regime at a pressure of 0.2 Torr to ensure accurate retrieval of the ILS. The analysis indicated that the ILS is best matched by a

Table 1. Experimental conditions (each scan takes approximately 3.5 h).

Lines scanned	Average cell temperature (K)	Temperature deviation during scan (K)	Average chamber gradiant ($K\,m^{-1}$)	Average pressure during scan (Torr)	Pressure deviation during scan (Torr)
R19 to R0	214.089	0.905	1.142	22.829	0.012
R19 to R0	214.179	0.856	1.107	36.939	0.016
R19 to R0	214.328	1.061	1.385	9.623	0.002
R19 to R0	233.459	0.407	0.485	40.189	0.012
R19 to R0	233.682	0.535	0.650	10.465	0.003
R19 to R0	233.729	0.529	0.646	24.866	0.001
R19 to R0	253.170	0.254	0.277	43.520	0.007
R19 to R0	253.235	0.286	0.319	26.908	0.005
R19 to R0	253.240	0.256	0.291	11.318	0.001
R19 to R0	272.811	0.135	0.049	10.342	0.001
R19 to R0	272.850	0.165	0.148	25.330	0.004
R19 to R0	272.933	0.163	0.209	40.635	0.002
R19 to R0	292.814	0.165	0.061	43.547	0.001
R19 to R0	292.824	0.164	0.069	27.149	0.001
R19 to R0	292.829	0.172	0.065	11.089	0.001
R19 to R0	312.797	0.192	0.025	40.482	0.003
R19 to R0	312.808	0.196	0.034	9.505	0.001
R19 to R0	312.820	0.202	0.054	24.261	0.001
R19 to R0	332.529	0.242	−0.111	42.992	0.001
R19 to R0	332.530	0.240	−0.108	10.093	0.001
R19 to R0	332.577	0.220	−0.062	25.774	0.002

Lorentz profile with a half-width of $8.167 \times 10^{-5}\text{cm}^{-1}\text{atm}^{-1}$. All spectral analyses presented in this study were completed by convolving the various line shape functions [28,29] with this ILS function.

All spectra were analysed using a multispectrum fit technique [30]. In order to determine a more realistic error associated with each line shape parameter, other than those provided by the fitting program, individual fits were performed on the R(7), R(10), R(13), R(16), R(18) and R(19) transitions of the $\nu_1+\nu_2+\nu_4+\nu_5$ band. For each pressure the spectra recorded for this set of transitions were fit using a Rautian line shape profile. The resulting pressure-dependent coefficients were then plotted against the pressure to determine the pressure-independent coefficient. This method allowed us to determine the error associated with each pressure-independent coefficient. In the case of self-broadening we found the measurement errors to be no greater the 1%, for self-shifts they were found to be no greater than 4.5% and for narrowing they were no larger than 3%. These errors have been quoted in all tables listed below.

3. Spectroscopic line shape analysis

By carefully examining the absorption of incident radiation as it travels though the gas sample we can determine the values for the various coefficients used with the designated line shape model. First we start by using the Beer–Lambert law for absorption due to a monochromatic source:

$$\left(\frac{I_t}{I_0}\right)_\nu = \mathrm{e}^{-\alpha_\nu} \tag{1}$$

Here I_t and I_0 represent transmitted and incident laser intensities. The absorbance α_ν can be further decomposed into the following form:

$$\alpha_\nu = P\chi_{\text{abs}}S(T)\varphi_\nu L \tag{2}$$

Here P is the pressure in atmospheres, χ_{abs} is the mole fraction of the absorbing species, T is the gas temperature in Kelvin, S is the line strength in $\text{cm}^{-2}\text{atm}^{-1}$, and φ_ν is the line shape function.

The choice of line shape function φ_ν depends greatly on the physical conditions of the gas being examined. Two main broadening mechanisms can generally be used to describe the line shape of a spectral line. The first is the Doppler width, which is the result of the thermal motion of the molecules. When the pressure is sufficiently low, any broadening due to intermolecular collisions can be neglected, resulting in a line shape that has a Gaussian shape with a half-width of γ_{D}. However, at higher pressures the effects due to intermolecular collisions become the leading contributor to the broadening of the line. At these higher pressures it then becomes necessary to employ the use of a Lorentz function to define the line shape which has a half-width of γ_{L}. For intermediate pressures a Voigt model is generally used to describe the line shape. The Voigt line shape model is the convolution of a Gaussian and Lorentz line shape and therefore contains the characteristic broadening components from both profiles. This results in a half-width that is a combination of the original two counterparts γ_{D} and γ_{L}.

For intermediate pressure the use of the Voigt function is only effective as long as the mean free path of the molecules is sufficiently large when compared with the wavelength of the incident radiation λ. If the mean free path becomes equal to or less than λ the resulting motion of the molecules then becomes Brownian in nature and thus the diffusion of the gas becomes relevant. The pressure regime for which this condition stands is referred to as the 'Dicke narrowing' regime and the associated line shapes are narrowed.

From the Brownian movement model [31] we can define the velocity of the molecule using the following equation:

$$\frac{\mathrm{d}u}{\mathrm{d}t} = -\beta u + A(t) \tag{3}$$

Here $\boldsymbol{u}$ is the velocity, the $\beta\boldsymbol{u}$ term represents the dynamic friction experienced by the molecule and $\boldsymbol{A}(t)$ is the characteristic random fluctuating portions associated with Brownian motion. In the Doppler pressure regime, the velocity of the molecules is defined strictly in terms of a Maxwellian distribution. However, from Equation (3) it can be seen that, outside the Doppler regime, the velocity is dependent on the frictional coefficient β. From this result it is evident that in order to describe the spectral line shape when the mean free path of the molecule of interest is equal to or less than λ we must employ special line shape profiles that contain within them this frictional coefficient.

The two most common models used to describe the Dicke narrowing regime are the Galatry [28] (soft collision model) and Rautian [29] (hard collision model) line shape functions. Figure 1 shows the results of fitting the R(13) line of the $\nu_1+\nu_2+\nu_4+\nu_5$ band using the Voigt, Galatry (soft) and Rautian (hard) line shape models. It is clear from Figure 1 that we are in the Dicke narrowing regime, as it can be seen that we obtain a 'w'-type residual when the spectral feature is fit using a Voigt profile. What is not immediately clear is whether the Soft or Hard collision model is a better choice for modeling these features. Therefore,

a complete analysis was performed using both Galatry and Rautian line shape models.

Below we present the expressions used to retrieve the self-broadened half-width and pressure-induced shift coefficients and their temperature dependences:

$$\gamma(p,T) = p\gamma^0(p_0,T_0)\left[\frac{T_0}{T}\right]^n \quad (4)$$

$$\upsilon = \upsilon_0 + p\delta^0 \quad (5)$$

$$\delta^0 = \delta^0(T_0) + \delta'(T - T_0) \quad (6)$$

In Equations (4)–(6) the reference pressure and temperature are $p_0 = 1$ atm and $T_0 = 296$ K, respectively. γ^0 is the retrieved self-broadened half-width coefficient at the reference pressure p_0 (1 atm) and reference temperature T_0 (296 K). γ is the measured self-broadened half-width coefficient of the spectral line and p is the total sample pressure in atmospheres. n is the temperature dependence exponent of the self-broadened half-width coefficient. δ^0 is the pressure-induced shift coefficient, υ is the measured line position, υ_o is the position at zero pressure, and δ' is the temperature-dependent coefficient of the self-induced pressure shift coefficients.

Although the effects due to line mixing are not clearly evident at the pressures studied here, we have accounted for line mixing effects in our line shape modeling. In the weak line mixing regime, the spectral lines are slightly asymmetric. The line asymmetry was modeled in our analysis software by adding a dispersive profile of amplitude $pY_{0k}(T)$ to the non-dispersive Galatry or Rautian profiles, where p is the gas pressure in atm and $Y_{0k}(T)$ is the line mixing coefficient of the transition of interest. The line mixing coefficients for individual transitions are taken from our study published in Ref. [26].

Using both the Galatry and Rautian line shape models we examined the self- broadening, self-shift and narrowing parameters for 20 transitions in the $\nu_1 + \nu_2 + \nu_4 + \nu_5$ band of C_2H_2. The line parameters were obtained using weighted multispectrum analysis software [30]. Multispectrum fits were performed on spectra of varying pressures that were recorded at the same set temperature. Through the use of a nonlinear least squares fitting routine the line parameters were optimized by minimizing the residual. The initial parameter values for self-broadening and shift used in the fitting procedure were taken from Refs. [26,32].

3.1. *Self-broadening*

Using Equation (4) we determined the temperature dependence of the self-broadening coefficients. Table 2 shows the self-broadening coefficients that were obtained for both the Soft and Hard collision models at a temperature of 293 K. The table also shows the retrieved temperature dependence coefficients n.

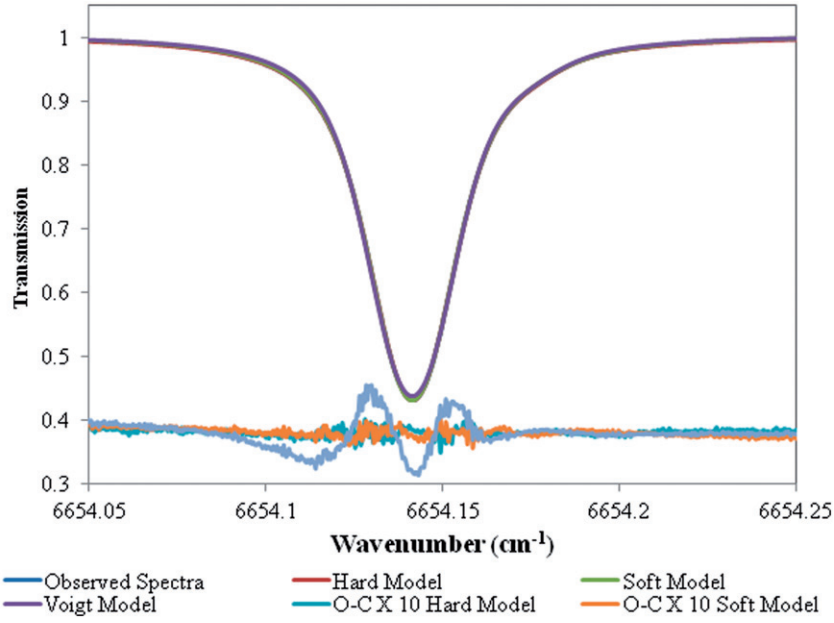

Figure 1. Observed and calculated spectra for the R(13) transition of the $\nu_1 + \nu_2 + \nu_4 + \nu_5$ band of C_2H_2. Here the residuals have been shifted and magnified for easier comparison.

Figure 2 shows the self-broadening coefficients that were obtained from spectra recorded at 293 K. The results indicate very close agreement with both theoretical calculations completed by Bouanich and Predoi-Cross [33] and our previous analysis [26] completed using a Voigt profile. A further comparison with many of the preceding studies is given in Figure 3. It is clear from this figure that our obtained self-broadening coefficients at 293 K are in agreement with the majority of the experimental results in the last decade or so.

Table 2. Self-broadening coefficients at 293 K and temperature-dependentcoefficients n for both the Soft and Hard collision line shape models.

Line	m	Soft γ_0	Soft n	Hard γ_0	Hard n
R(0)	1	0.219(2)	0.63(7)	0.218(2)	0.65(7)
R(1)	2	0.196(2)	0.70(1)	0.194(2)	0.71(1)
R(2)	3	0.182(2)	0.77(3)	0.180(2)	0.78(3)
R(3)	4	0.177(2)	0.65(1)	0.176(2)	0.66(1)
R(4)	5	0.167(2)	0.69(1)	0.165(2)	0.70(1)
R(5)	6	0.165(2)	0.68(2)	0.163(2)	0.70(1)
R(6)	7	0.159(2)	0.72(2)	0.157(2)	0.73(2)
R(7)	8	0.158(2)	0.68(1)	0.157(2)	0.69(1)
R(8)	9	0.154(2)	0.70(1)	0.153(2)	0.71(1)
R(9)	10	0.154(2)	0.71(2)	0.153(2)	0.72(2)
R(10)	11	0.150(1)	0.72(2)	0.148(1)	0.74(2)
R(11)	12	0.151(2)	0.68(1)	0.150(1)	0.69(1)
R(12)	13	0.148(1)	0.64(1)	0.147(1)	0.65(1)
R(13)	14	0.143(1)	0.64(1)	0.142(1)	0.65(1)
R(14)	15	0.138(1)	0.66(2)	0.137(1)	0.67(2)
R(15)	16	0.137(1)	0.61(1)	0.136(1)	0.62(1)
R(16)	17	0.133(1)	0.60(2)	0.132(1)	0.62(2)
R(17)	18	0.132(1)	0.51(1)	0.130(1)	0.56(1)
R(18)	19	0.124(1)	0.59(2)	0.122(1)	0.60(1)
R(19)	20	0.124(1)	0.56(2)	0.123(1)	0.57(2)

The general trend of the temperature-dependent coefficients can be seen in Figure 4. It was found that, for the Soft and Hard collision models, we obtained on average larger values for n than those obtained from Ref. [26]. We also found that we had better agreement with the semi-classical calculations completed by Bouanich and Predoi-Cross [33]. Figure 4 also indicates that our previous Voigt results match well with the Voigt results obtained by Dyne *et al.* [14]. However, the results from the Soft and Hard profiles do not agree as well. The results obtained by Dyne *et al.* [14] for the Soft and Hard profiles were found to be in close agreement with their results using the Voigt profile. We would assume that we should have also obtained a similar result when comparing the three different line shape models. This is not the case with our observed results for the temperature dependence coefficient. The slightly increased values of n may be due to the determination of the narrowing parameter. Therefore, a direct comparison of our Soft and Hard line shape results with those of Dyne *et al.* [14] may not be appropriate.

3.2. *Self-shift*

The self-shift δ and temperature-dependent coefficients δ' were determined using Equations (5) and (6).

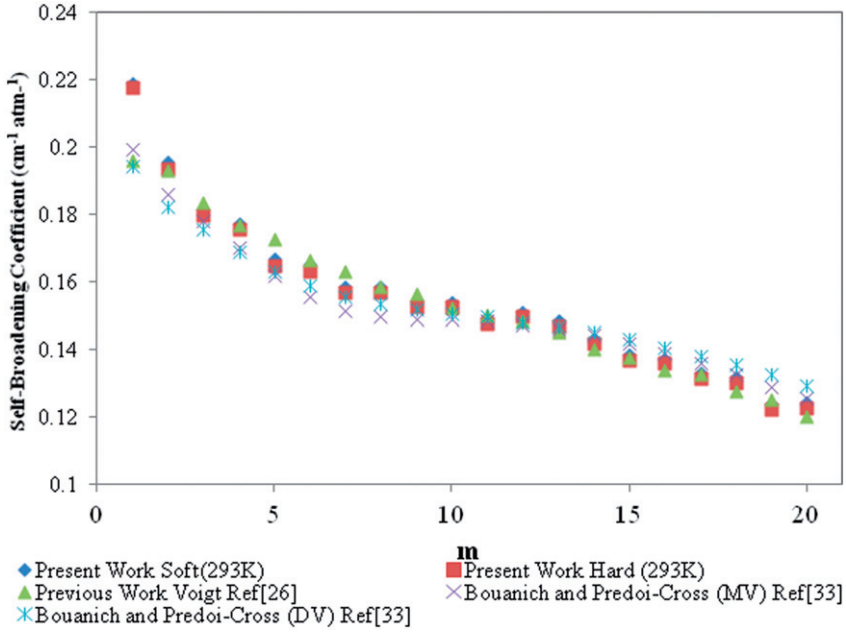

Figure 2. Self-broadening coefficients at 293 K.

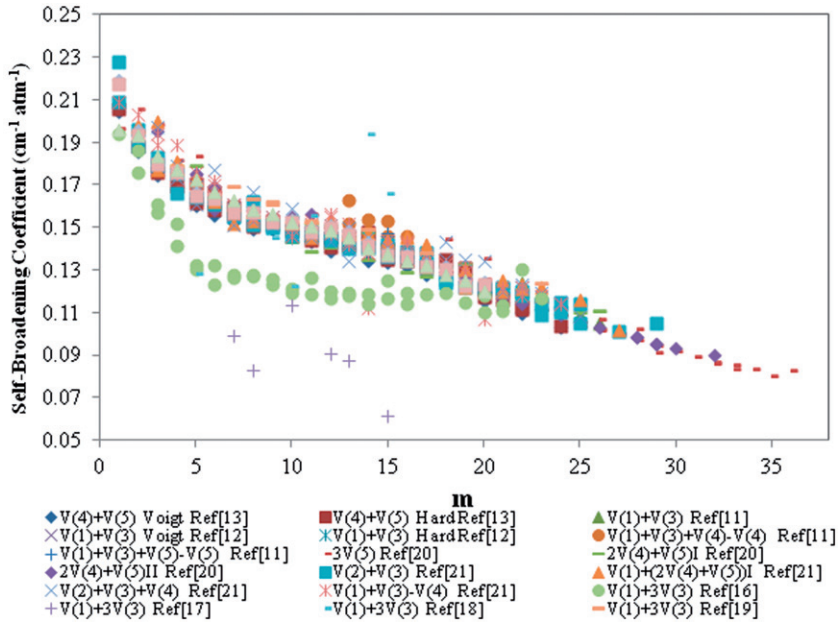

Figure 3. Comparison of self-broadening coefficients from previous studies.

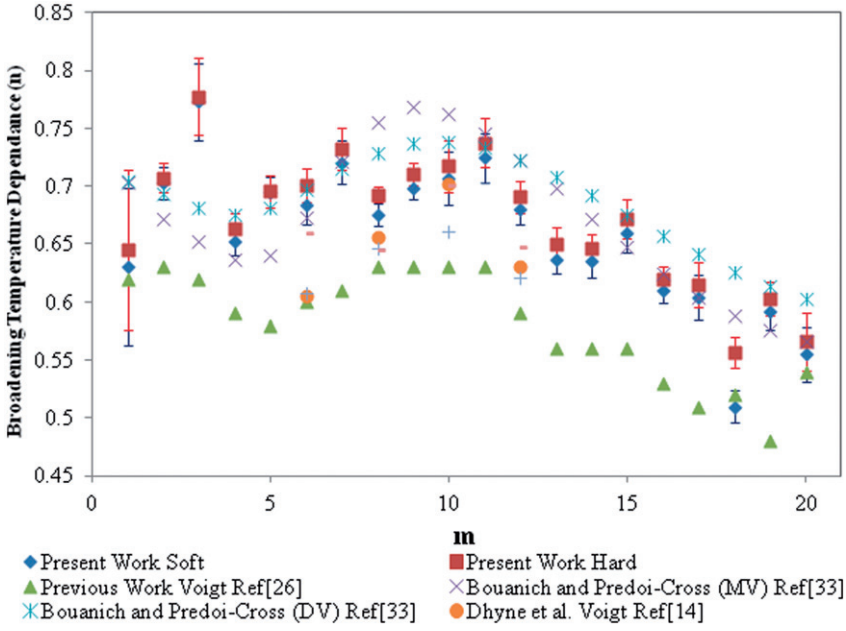

Figure 4. Temperature dependence coefficients n obtained from Equation (4).

Table 3 and Figure 5 show the self-shift coefficients obtained from both the Soft and Hard line shape models for spectra recorded at 293 K. Figure 5 shows good agreement with the semi-classical calculations obtained by Bouanich and Predoi-Cross [33] and also agree well with our previous work [26] using a Voigt profile.

The self-shift temperature-dependent coefficient δ' is given in Table 3 and Figure 6. The figure indicates that δ' has rotational dependence. This same dependence was observed using a Voigt profile in our previous work [26], but has also been calculated in theoretical calculations preformed by Bouanich and Predoi-Cross [33]. It is also very important to note that

we tried to examine a second-order expression as proposed by Bouanich and Predoi-Cross [33], but found that the errors in our shift coefficients were too large to make an accurate assessment of the δ'' term proposed.

Table 3. Self-shift coefficients at 293 K and temperature-dependent coefficients δ' for both the Soft and Hard collision line shape models.

Line	m	Soft δ_0 (10^{-3})	δ' (10^{-5})	Hard δ_0 (10^{-3})	δ' (10^{-5})
R(0)	1	−3.9(2)	−5.3(9)	−3.9(2)	−5.3(9)
R(1)	2	0.6(1)	−1.2(3)	0.4(1)	−2.8(2)
R(2)	3	−1.4(1)	−2.8(1)	−1.4(1)	−2.8(1)
R(3)	4	−1.4(1)	0.7(2)	−1.4(1)	0.7(2)
R(4)	5	−1.3(1)	2.4(5)	−1.3(1)	2.4(5)
R(5)	6	−3.0(1)	1.1(1)	−3.0(1)	1.1(1)
R(6)	7	−3.2(1)	1.1(1)	−3.3(1)	1.1(1)
R(7)	8	−4.2(2)	1.6(2)	−4.2(2)	1.6(2)
R(8)	9	−5.1(2)	1.2(2)	−5.1(2)	1.2(2)
R(9)	10	−5.3(2)	3.8(5)	−4.9(2)	4.2(5)
R(10)	11	−5.6(3)	2.8(4)	−5.6(3)	2.8(4)
R(11)	12	−6.0(3)	2.9(2)	−6.0(3)	2.9(2)
R(12)	13	−6.7(3)	3.0(3)	−6.7(3)	3.0(3)
R(13)	14	−7.0(3)	3.6(2)	−7.0(3)	3.6(2)
R(14)	15	−8.2(4)	2.8(4)	−8.2(4)	2.8(4)
R(15)	16	−8.3(4)	4.2(3)	−8.3(4)	4.2(3)
R(16)	17	−8.1(4)	4.3(4)	−8.1(4)	4.3(4)
R(17)	18	−9.1(4)	5.7(5)	−9.1(4)	5.7(5)
R(18)	19	−9.4(4)	3.0(3)	−9.4(4)	2.9(3)
R(19)	20	−10.1(5)	4.9(2)	−10.1(5)	4.9(2)

3.3. *Self-narrowing*

Building on the work completed by both Herregodts *et al*. [16] and Valipour and Zimmermann [19] we have measured the narrowing coefficients for both Soft and Hard collision models for acetylene. Initially, we recorded spectra ranging from 100 Torr down to 10 Torr and ranging in temperatures from 213 to 333 K. By carefully examining the pressure dependence of the narrowing coefficient we determined that only spectra recorded in the region of 40 to 10 Torr were within the Dicke narrowing regime. From these spectra we obtained for the first time the temperature dependence of the narrowing coefficients.

Recent work by Li *et al*. [34], examining narrowing in water vapor spectra, concluded that the temperature dependence of narrowing is similar to that of the temperature dependence of broadening. Figure 7 depicts the log of the narrowing coefficient for the R(11) transition and its relation to temperature. From the figure we see that it does indeed have a linear-type dependence, much like the broadening coefficient. Based on this reasoning and the work completed by Li *et al*. [34] we chose to use the following expression to describe the temperature dependence of the narrowing coefficients:

$$\beta(p, T) = p\beta^0(p_0, T_0)\left[\frac{T_0}{T}\right]^{n'} \tag{7}$$

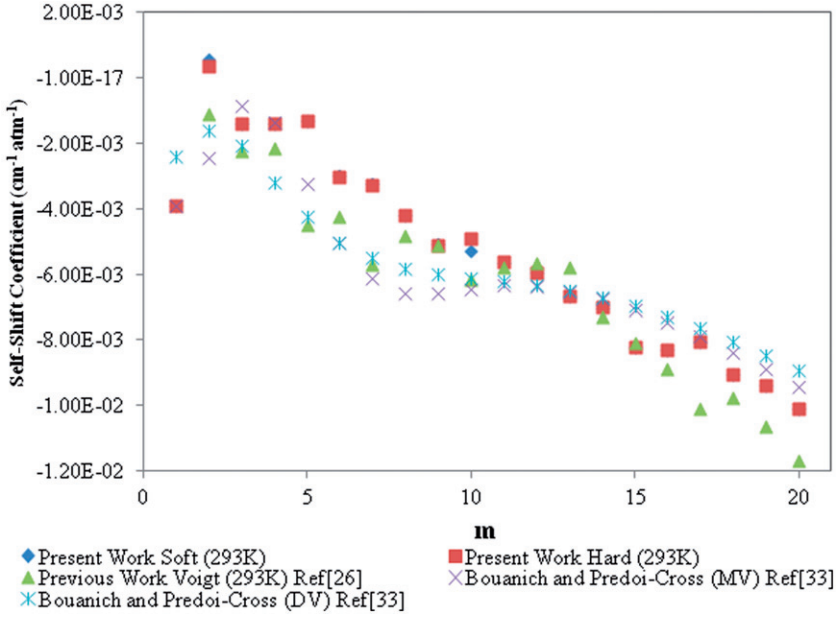

Figure 5. Self-shift coefficients obtained from spectra recorded at 293 K.

Here the reference pressure p_0 and temperature T_0 are defined the same as for Equations (4)–(6). β^0 is the retrieved self-narrowing coefficient at the reference pressure p_0 and reference temperature T_0. β is the measured self-narrowing coefficient of the spectral line and p is the total sample pressure in atmospheres. n' is the temperature dependence exponent of the self-narrowing coefficient.

Table 4 and Figure 8 show the narrowing coefficients obtained from spectra recorded at 293 K. From the figure we see that there is in fact a small rotational dependence associated with the narrowing coefficient. A similar trend was also observed by Valipour and Zimmermann [19] for the $\nu_1 + 3\nu_3$ band. From Figure 8 we see that our narrowing coefficients for the Hard collision model agree well with those of

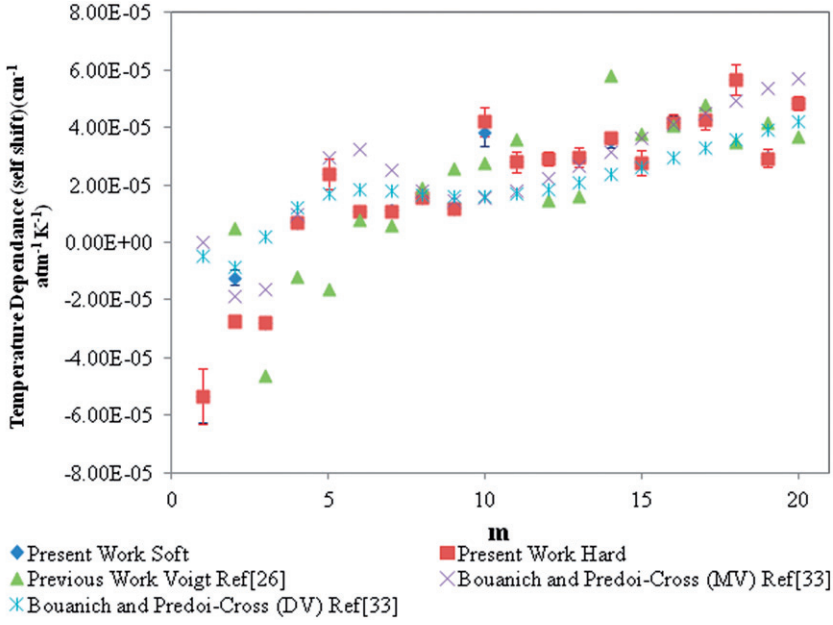

Figure 6. Temperature dependence term δ' obtained from Equation (6).

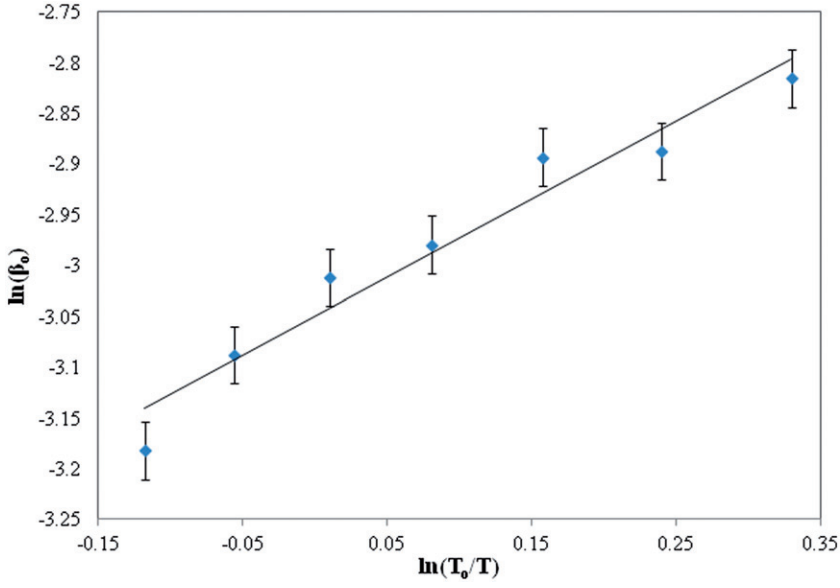

Figure 7. Careful examination of the R(11) transition relationship to variations in temperature.

Valipour and Zimmermann [19], but are on average slightly lower than those obtained by Herregodts *et al*. [16].

It was observed by Herregodts *et al*. [16] that the Soft collision model gave larger narrowing coefficients than the Hard collision model. However, due to the signal-to-noise ratio of their experiment they were unable to identify which model fit more appropriately. We also noticed this same trend, however with our improved signal-to-noise ratio we are still unable to justify the selection of one model over the other. It was found from the residuals of many fits for both models that there was no substantial difference between them and therefore no preferential model could be determined.

Table 4. Self-narrowing coefficients at 293 K and the temperature dependence coefficients n' for both the Soft and Hard collision line shape models.

Line	m	Soft β_0	n'	Hard β_0	n'
R(0)	1	0.099(3)	−0.5(2)	0.076(2)	2.4(2)
R(1)	2	0.087(3)	1.0(1)	0.063(2)	1.1(1)
R(2)	3	0.078(2)	1.5(2)	0.058(2)	1.6(2)
R(3)	4	0.084(3)	0.6(1)	0.063(2)	0.7(1)
R(4)	5	0.070(2)	1.6(3)	0.050(2)	1.7(2)
R(5)	6	0.081(2)	0.5(1)	0.060(2)	0.7(1)
R(6)	7	0.069(2)	0.9(2)	0.050(2)	1.1(2)
R(7)	8	0.068(2)	0.4(2)	0.052(2)	0.6(1)
R(8)	9	0.064(2)	0.7(1)	0.047(1)	0.8(1)
R(9)	10	0.061(2)	0.6(1)	0.044(1)	0.7(1)
R(10)	11	0.066(2)	0.8(2)	0.048(1)	0.7(2)
R(11)	12	0.065(2)	0.6(1)	0.049(1)	0.8(1)
R(12)	13	0.062(2)	0.6(1)	0.045(1)	0.7(1)
R(13)	14	0.052(2)	0.6(2)	0.039(1)	0.7(2)
R(14)	15	0.056(2)	0.6(1)	0.040(1)	0.8(1)
R(15)	16	0.051(2)	0.7(1)	0.038(1)	0.8(1)
R(16)	17	0.054(2)	0.7(1)	0.039(1)	0.9(1)
R(17)	18	0.056(2)	0.4(1)	0.040(1)	0.8(2)
R(18)	19	0.046(1)	0.6(1)	0.032(1)	0.7(1)
R(19)	20	0.048(1)	0.8(2)	0.034(1)	0.9(2)

The temperature dependence term n' from Equation (7) was also determined and is presented in Table 4 and shown in Figure 9. The temperature dependence coefficient n' was found to be similar between both types of models. The largest difference in n' was found for the R(0) transition and is most likely due to the low intensity of the transition and the more intense neighboring features. The larger variation in n' that is seen for transitions R(0) to R(10) may be the result of undefined neighboring spectral features. Similar unidentified features were also observed by Li *et al*. [12] in this region and can be attributed to unassigned hot bands with very small intensity. Every attempt was made to incorporate these features into the fitting routine, however without more information the spectral parameters used may not have been the ideal values for these unknown transitions.

3.4. *Diffusion coefficients*

Herregodts *et al*. [16] found that the values they had obtained agreed well with the dynamic friction coefficient $\beta^0_{\text{diff}} = 37.8(3) \times 10^{-3}\,\text{cm}^{-1}/\text{atm}$ determined

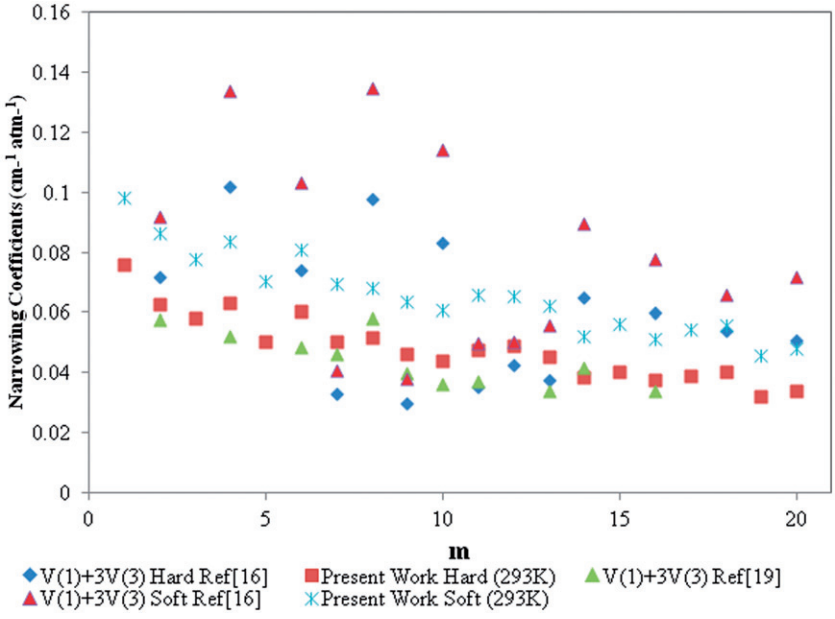

Figure 8. Narrowing coefficients obtained from multispectral fitting of spectra recorded at 293 K.

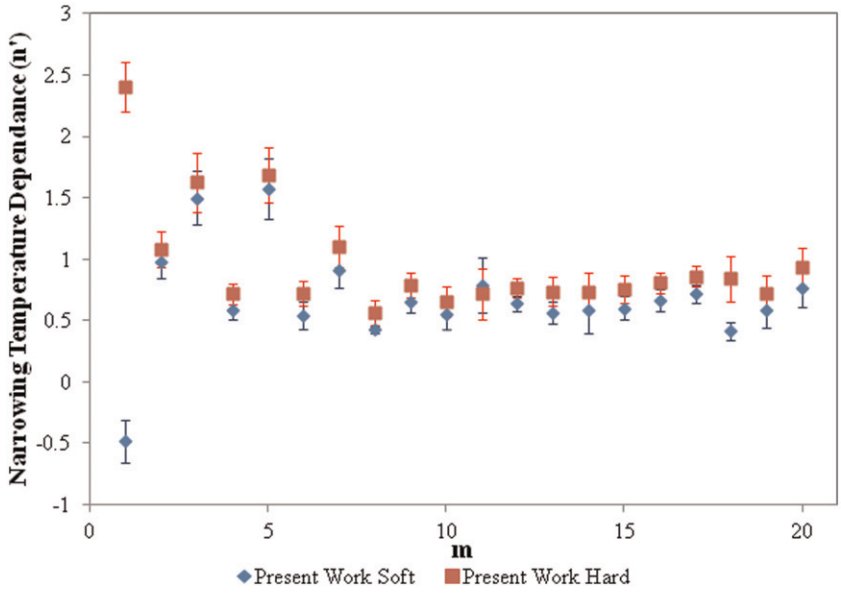

Figure 9. Narrowing temperature dependence coefficient n' obtained from Equation (7).

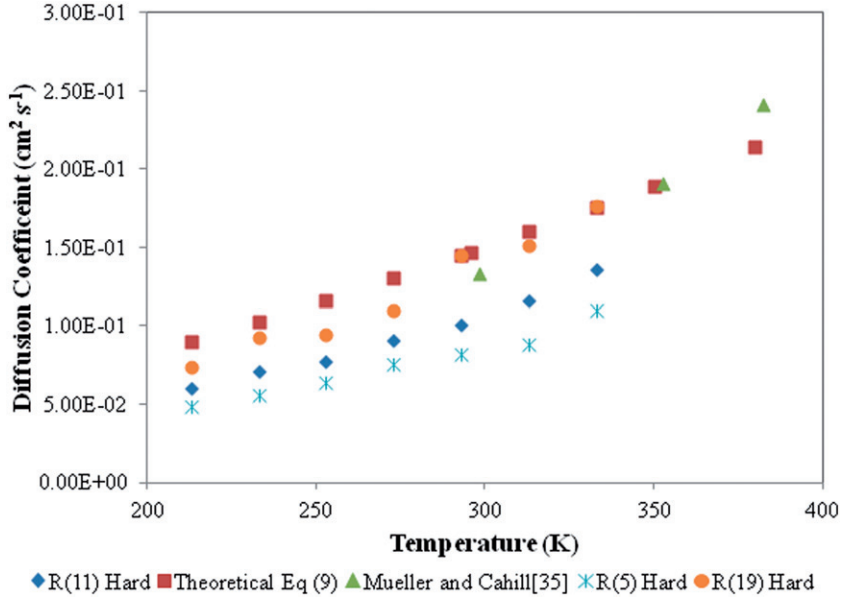

Figure 10. Comparison of diffusion coefficients. The diffusion coefficients obtained for R(19), R(13) and R(11) were obtained through the use of Equation (8). The theoretical values were obtained from Equation (9).

experimentally by Mueller and Cahill [35]. Based on the relative agreement of our data with both Valipour and Zimmermann [19] and Herregodts *et al.* [16] we equated the narrowing parameter β^0 to the dynamic friction coefficient β^0_{diff} in an attempt to examine the diffusion coefficient and its temperature dependence. The dynamic friction coefficient β^0_{diff} can be determined by the following equation [34,36]:

$$\beta^0_{\text{diff}} = \frac{KT}{2\pi mcD_{11}} \tag{8}$$

Here K is the Boltzmann constant, T the temperature in Kelvin, m the mass of acetylene, c the speed of

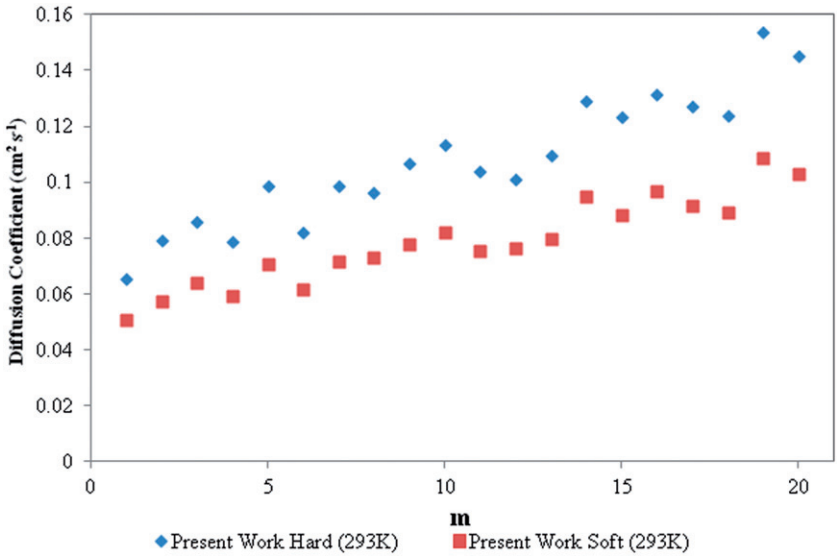

Figure 11. Experimentally determined diffusion coefficients obtained from retrieved β_0 at 293 K.

light and D_{11} is the self-diffusion coefficient for acetylene.

The diffusion coefficient for any gas may be obtained in a general sense using the following equation [37]:

$$D = 2.628 * 10^{-3}\left[\frac{\sqrt{T_3/M}}{p\sigma^2}\right](\mathrm{cm}^2/\mathrm{s}) \qquad (9)$$

Here M is the molecular weight, T the temperature in Kelvin, p the pressure in atmospheres and σ the molecular diameter in Ångstroms (for acetylene we used $\sigma = 4.221$ Å [38]).

Using Equation (8) we compared our experimentally determined diffusion coefficients with those obtained from Equation (9). Figure 10 shows the results of this comparison for three different transitions. It can be seen that both the experimental results and the theoretically determined equations share very similar slopes with temperature. This indicates very good agreement between our conceived notion of the diffusion coefficients' temperature dependence and what can actually be observed. Also seen in the figure are the results obtained by Mueller and Cahill [35] and they agree quite well with the results obtained from Equations (8) and (9). We can also see from the figure that the diffusion coefficient does in fact have a rotational dependence. It has been found that, as m increases, so too does the value of the diffusion coefficient. Figure 11 shows the diffusion coefficients and the rotational dependence obtained from spectra recorded at 293 K.

4. Conclusion

Using spectra recorded on our three-channel tunable diode laser system we have identified and re-confirmed spectral parameters for transitions in the $\nu_1 + \nu_2 + \nu_4 + \nu_5$ band of acetylene. The results obtained from completing detailed multi-spectral analysis on our data have indicated a very high agreement with most of the previous studies completed to date.

In this study we have for the first time examined the effect of temperature on the Dicke narrowing parameters obtained from two distinct line shape models (Galatry and Rautian). It was further found that we obtain a high level of agreement with both theory and other experimental results if we equate our narrowing parameters to that of the dynamic frictional coefficient obtained from the Brownian model. Furthermore, we have found that the narrowing coefficient and therefore also the diffusion coefficient do indeed have a rotational dependence.

With an even larger signal-to-noise ratio than that of Herregodts *et al.* [16] and Valipour and Zimmermann [19] we still have been unable to determine which line shape model best describes self-interacting acetylene.

References

[1] C.A. Nixon, R.K. Achterberg, P.N. Romani, M. Allen, X. Zhang, N.A. Teanby, P.G.J. Irwin and F.M. Flasar, Planet. Space Sci. **58**, 1667 (2010).

[2] T. Kostiuk, T. Hewagama, K.E. Fast, T.A. Livengood, J. Armen, D. Buhl, G. Sonnabend, F. Schmulling, J.D. Delgado and R. Achterberg, Planet. Space Sci. **58**, 1715 (2010).
[3] A. Coustenis, R.K. Achterberg, B.J. Conrath, D.E. Jennings, A. Marten, D. Gautier, C.A. Nixon, F.M. Flasar, N.A. Teanby, B. Bézard, R.E. Samuelson, R.C. Carlson, E. Lellouch, G.L. Bjoraker, P.N. Romani, F.W. Taylor, P.G.J. Irwin, T. Fouchet, A. Hubert, G.S. Orton, V.G. Kunde, S. Vinatier, J. Mondellini, M.M. Abbas and R. Courtin, Icarus **189**, 35 (2007).
[4] T. Fouchet, E. Lellouch, B. Bézard, H. Feuchtgruber, P. Drossart and T. Encrenaz, Astron. Astrophys. **355**, L13 (2000).
[5] H.W.M.A.J.T. Clarke, Astrophys. J. **229**, L107 (1979).
[6] D. Cronn and E. Robinson, Geophys. Res. Lett. **6**, 641 (1979).
[7] A. Goldman, F.J. Murcray, R.D. Blatherwick, J.R. Gillis, F.S. Bonomo, F.H. Murcray, D.G. Murcray and R.J. Cicerone, J. Geophys. Res.–Oceans Atmos. **86**, 2143 (1981).
[8] R. Zander, C.P. Rinsland, D.H. Ehhalt, J. Rudolph and P. Demoulin, J. Atmos. Chem. **13**, 359 (1991).
[9] J. Rudolph, A. Khedim and B. Bonsang, J. Geophys. Res.–Atmos. **97**, 6181 (1992).
[10] P. Varanasi and B.R.P. Bangaru, J. Quantit. Spectros. Radiat. Trans. **15**, 267 (1975).
[11] P. Minutolo, C. Corsi, F. D'Amato and M. De Rosa, Eur. Phys. J. D **17**, 175 (2001).
[12] J.S. Li, G. Durry, J. Cousin, L. Joly, B. Parvitte and V. Zeninari, J. Quantit. Spectrosc. Radiat. Trans. **111**, 2332 (2010).
[13] M. Lepère, G. Blanquet, J. Walrand, J.P. Bouanich, M. Herman and J.V. Auwera, J. Molec. Spectrosc. **242**, 25 (2007).
[14] M. Dhyne, P. Joubert, J.C. Populaire and M. Lepère, J. Quantit. Spectrosc. Radiat. Trans. **112**, 969 (2011).
[15] A. Lucchesini, M. DeRosa, D. Pelliccia, A. Ciucci, C. Gabbanini and S. Gozzini, Appl. Phys. B–Lasers Opt. **63**, 277 (1996).
[16] F. Herregodts, D. Hurtmans, J. Vander Auwera and M. Herman, J. Chem. Phys. **111**, 7954 (1999).
[17] D. Biswas, B. Ray, S. Dutta and P.N. Ghosh, Appl. Phys. B–Lasers Opt. **68**, 1125 (1999).
[18] C. Yelleswarapu and A. Sharma, J. Quantit. Spectros. Radiat. Trans. **69**, 151 (2001).
[19] H. Valipour and D. Zimmermann, J. Chem. Phys. **114**, 3535 (2001).
[20] D. Jacquemart, J.Y. Mandin, V. Dana, L. Regalia-Jarlot, X. Thomas and P. Von der Heyden, J. Quantit. Spectrosc. Radiat. Trans. **75**, 397 (2002).
[21] O.M. Lyulin, D. Jacquemart, N. Lacome, V.I. Perevalov and J.Y. Mandin, J. Quantit. Spectrosc. Radiat. Trans. **109**, 1856 (2008).
[22] J.S. Wong and J. Molec, Spectrosc. **82**, 449 (1980).
[23] R. Georges, D. VanderVorst, M. Herman and D. Hurtmans, J. Molec. Spectrosc. **185**, 187 (1997).
[24] A.S. Pine, J. Quantit. Spectrosc. Radiat. Trans. **50**, 149 (1993).
[25] D. Lambot, J.C. Populaire, J. Walrand, G. Blanquet and J.P. Bouanich, J. Molec. Spectrosc. **165**, 1 (1994).
[26] C. Povey, A. Predoi-Cross and D.R. Hurtmans, J. Molec. Spectrosc. **268**, 177 (2011).
[27] J.Y. Wang, P. Ehlers, I. Silander and O. Axner, J. Opt. Soc. Am. B–Opt. Phys. **28**, 2390 (2011).
[28] L. Galatry, Phys. Rev. **122**, 1218 (1961).
[29] S.G. Rautian and I.I. Sobelman, Sov. Phys. Uspekhi-Ussr **9**, 701 (1967).
[30] D. Hurtmans, G. Dufour, W. Bell, A. Henry, A. Valentin and C. Camy-Peyret, J. Molec. Spectrosc. **215**, 128 (2002).
[31] S. Chandrasekhar, Rev. Mod. Phys. **15**, 0001 (1943).
[32] L.S. Rothman, I.E. Gordon, A. Barbe, D.C. Benner, P.E. Bernath, M. Birk, V. Boudon, L.R. Brown, A. Campargue, J.P. Champion, K. Chance, L.H. Coudert, V. Dana, V.M. Devi, S. Fally, J.M. Flaud, R.R. Gamache, A. Goldman, D. Jacquemart, I. Kleiner, N. Lacome, W.J. Lafferty, J.Y. Mandin, S.T. Massie, S.N. Mikhailenko, C.E. Miller, N. Moazzen-Ahmadi, O.V. Naumenko, A.V. Nikitin, J. Orphal, V.I. Perevalov, A. Perrin, A. Predoi-Cross, C.P. Rinsland, M. Rotger, M. Simeckova, M.A.H. Smith, K. Sung, S.A. Tashkun, J. Tennyson, R.A. Toth, A.C. Vandaele and J. Vander Auwera, J. Quantit. Spectrosc. Radiat. Trans. **110**, 533 (2009).
[33] J.P. Bouanich and A. Predoi-Cross, Molec. Phys. **109**, 2071 (2011).
[34] H. Li, A. Farooq, J.B. Jeffries and R.K. Hanson, Appl. Phys. B–Lasers Opt. **89**, 407 (2007).
[35] C.R. Mueller and R.W. Cahill, J. Chem. Phys. **40**, 651 (1964).
[36] M. Lepère, A. Henry, A. Valentin and C. Camy-Peyret, J. Molec. Spectrosc. **208**, 25 (2001).
[37] J.O. Hirschfelder, C.F. Curtiss and R.B. Bird, *Molecular Theory of Gases and Liquids* (Wiley–Interscience, New York, 1964), p. 1280.
[38] T. Titani, Chem. Soc. Jpn **5**, 98 (1930).